AIP Advances

Direct evaluation method to measure permittivity and conductivity of thin layers via wave approach in the THz region

Cite as: AIP Advances **9**, 115113 (2019); https://doi.org/10.1063/1.5115092
Submitted: 14 June 2019 • Accepted: 29 October 2019 • Published Online: 20 November 2019

Yunsang Kwak, Sang Mok Park, Sinyeob Lee, et al.

Direct evaluation method to measure permittivity and conductivity of thin layers via wave approach in the THz region

Cite as: AIP Advances 9, 115113 (2019); doi: 10.1063/1.5115092
Submitted: 14 June 2019 • Accepted: 29 October 2019 •
Published Online: 20 November 2019

Yunsang Kwak,[1] Sang Mok Park,[1] Sinyeob Lee,[2] Hak-Sung Kim,[1] Ju Lee,[3] and Junhong Park[1,a)]

AFFILIATIONS

[1]Department of Mechanical Engineering, Hanyang University, 222 Wangsimni-ro, Seongdong-gu, Seoul 04763, South Korea
[2]Samsung Electronics Co., 158 Baebang-ro, Asan-si, Chungcheongnam-do 31489, South Korea
[3]Department of Electrical Engineering, Hanyang University, 222 Wangsimni-ro, Seongdong-gu, Seoul 04763, South Korea

[a)]Author to whom correspondence should be addressed: parkj@hanyang.ac.kr

ABSTRACT

The direct evaluation method for measuring the permittivity and conductivity of thin layers was proposed via the wave approach in the terahertz (THz) region. The terahertz time-domain spectroscopy (THz-TDS) was employed for performing experiments with thin dielectric layers. The proposed method takes advantage of the wave prediction for propagated THz waves in the thin layer. The transient and spectral responses of the THz waves propagated in the thin layer were predicted directly through the proposed wave approach. The numerical procedures utilizing the predicted waves were presented to derive the complex wavenumber in the THz region, which is composed of the permittivity and conductivity. The derived properties were verified by comparing with the measured behaviors in time and frequency domains. The proposed numerical procedures allow us to measure precisely the complex dielectric property of the thin layer without any pre-estimation for layer inner conditions.

I. INTRODUCTION

When electromagnetic waves are interacted with an object, changes in their magnitude and phase can be used to infer the material properties of the object.[1–4] Many noncontact methods to measure the properties have been developed by analyzing reflected microwaves along intended paths.[5,6] Several researchers presented the measurement methods by utilizing the quality factor of resonances[7,8] and the waveguide[9] and free-space method.[10] The previous methods based on wave detection require specific sample conditions and calibrations. Implementations of the methods in a higher frequency region inevitably required further considerations in terms of wavenumber and speed due to their sophisticated signal manipulations, showing limitation on practical applications.[11,12]

Terahertz time-domain spectroscopy (THz-TDS) has exhibited remarkable performance in nondestructive evaluation of various materials.[13–16] The terahertz (THz) waves have advantages of high penetrability with low photon energy, do not require a liquid couplant, and are harmless to humans.[17–19] These features enable efficient implementations to be achieved for the noncontact and real-time evaluating method.[20–22] Due to the advantages of the THz waves, there has been strong interest in the measurement of the electromagnetic properties in the THz region by utilizing the refractive index of temporal echoes of THz waves.[23–29] These echo methods were performed under the premise that the reflections do not interfere with each other, requiring an essential prerequisite to estimate transmission and reflection pathways.[30,31] The accurate prediction of the properties in the THz region deeply relied on the effective design of optical instruments, which require high experimental costs.

The originality of the proposed method lies in the theoretical approach utilizing the complex wavenumber in the THz region, reducing experimental costs without the further manipulation techniques. In this study, the proposed method takes advantage of a direct wave prediction for propagated THz waves through thin layers. The wave approach allows us to measure precisely two

electromagnetic properties (permittivity and conductivity) of layered materials and polymers in a direct manner without any pre-estimation and regressions, presenting a supplementary tool to analyze wave-behaviors measured from the THz-TDS. The THz pulse waves were measured after propagation through the thin layers by using the THz-TDS equipment. The transfer function in the THz region was predicted to analyze the frequency-dependent variation of the complex wavenumber, which is composed of the permittivity and conductivity. The complex wavenumbers of the thin layers were derived through the numerical procedure based on the wave predictions. The derived properties were verified by comparing with the measured THz behaviors in time and frequency domains. Given the direct approach to the propagated THz waves, the proposed method is straightforward to measure the properties of the thin layers with wider applications and optimized costs.

II. WAVE APPROACH TO ANALYZE THE TRANSFER FUNCTION OF THIN LAYERS

The propagation of the THz wave was predicted based on Maxwell's equations. For a source-free, homogeneous, and lossy medium, the wave propagations are predicted as[32,33]

$$\nabla \times \overline{E} = -i\omega\mu\overline{H}, \quad \nabla \times \overline{H} = i\omega\varepsilon\overline{E} + \overline{J}, \quad \nabla \cdot \left(\varepsilon\overline{E}\right) = 0, \quad \nabla \cdot \left(\mu\overline{H}\right) = 0, \tag{1}$$

where $\overline{E}$ is the electric intensity; $\overline{H}$ is the magnetic intensity; ε and μ are the permittivity and permeability of the medium, respectively; $\overline{J} = \sigma\overline{E}$ is the current density; and σ is the conductivity of the medium. The two-dimensional Helmholtz equation for a transverse electric wave derived by from Eq. (1) is given as follows:

$$\left(\nabla^2 + \omega^2\mu\hat{\varepsilon}_c\right)\overline{E} = 0, \tag{2}$$

where ω is the angular frequency and $\hat{\varepsilon}_c = \varepsilon(1 - i \cdot \sigma/\omega\varepsilon)$ is the complex permittivity. In order to predict the wave transfer in the pitch–catch mode, the propagated and reflected waves were divided in the medium of air and the thin layer. Assuming harmonic solution, $\overline{E} = \mathrm{Re}\left\{\hat{E}(x,z)e^{i\omega t}\right\}$, general wave solutions in the two layers are as follows:

$$\begin{aligned}\hat{E}_1(x,z) &= \hat{A}_1 e^{-i\hat{k}_{1x}\cdot x - i\hat{k}_{1z}\cdot z} + \hat{A}_2 e^{-i\hat{k}_{1x}\cdot x + i\hat{k}_{1z}\cdot z},\\ \hat{E}_2(x,z) &= \hat{A}_3 e^{-i\hat{k}_{2x}\cdot x - i\hat{k}_{2z}\cdot (z-L_0)} + \hat{A}_4 e^{-i\hat{k}_{2x}\cdot x + i\hat{k}_{2z}\cdot (z-L_0)},\end{aligned} \tag{3}$$

where $\hat{E}_1$ and $\hat{E}_2$ are the THz waves in air and the thin layer, respectively, and $\hat{k}_x$ and $\hat{k}_z$ are the wavenumbers in the x- and z-directions, respectively. $\hat{k}_1 = \omega\sqrt{\mu_1\hat{\varepsilon}_{c1}}$ and $\hat{k}_2 = \omega\sqrt{\mu_2\hat{\varepsilon}_{c2}}$ are the wavenumbers in air and the thin layer, respectively. $\hat{A}_n$ are the complex amplitudes, and L_o is the length from the emitter to the thin layer. The coordinates are shown in Fig. 1(b). The oblique incident THz wave from the emitter, $\hat{E}_I(x,z) = \hat{\alpha}_0 e^{-i\hat{k}_{1x}\cdot x - i\hat{k}_{1z}\cdot z}$, satisfies the following condition at $z = z_0$:

$$\hat{A}_1 e^{-i\hat{k}_{1x}\cdot x} = \hat{E}_I(z_0). \tag{4}$$

The mirror located at the bottom of the thin layer completely reflects the THz waves. The boundary condition at the layer bottom ($z = L + L_0$) is applied as follows:

$$\hat{E}_2(L + L_0) = 0, \tag{5}$$

where L is the layer thickness. At the interface between the two media, the THz waves follow the electric and magnetic continuity conditions (Snell's law) at $z = L_0$ as follows:

$$\hat{E}_1(L_0) = \hat{E}_2(L_0), \quad \mu_2 \cdot \partial\hat{E}_1(L_0)/\partial z = \mu_1 \cdot \partial\hat{E}_2(L_0)/\partial z. \tag{6}$$

The complex amplitudes of the wave solutions were obtained by symbolic analysis of the boundary conditions. The transfer function of the pitch–catch mode is calculated as follows:

$$\Lambda e^{i\phi} = \hat{E}_R(z_0)/\hat{E}_I(z_0), \tag{7}$$

where $\hat{E}_R(x,z) = \hat{A}_2 e^{-i\hat{k}_{1x}\cdot x + i\hat{k}_{1z}\cdot z}$ is the wave detected by the THz receiver, Λ is the magnitude, and ϕ is the phase of the transfer function.

The complex permittivity of the layer was derived to solve Eq. (7) with respect to the complex wavenumber. In order to numerically obtain the complex wavenumber of the thin layer, the Newton-Raphson iterations were performed as follows:[34]

$$\left(\partial\hat{E}_R(z_0)/\partial\hat{k}_2\right) \cdot \Delta\hat{k}_2 = \hat{E}_R(z_0) - \hat{E}_I(z_0)\Lambda e^{i\phi}. \tag{8}$$

The permeability of the dielectric layer was the same as that of air, and thus, the complex permittivity was calculated by using the wavenumber derived from the numerical process as follows:

$$\hat{\varepsilon}_c = \hat{k}_2^2/\mu_0\omega^2, \tag{9}$$

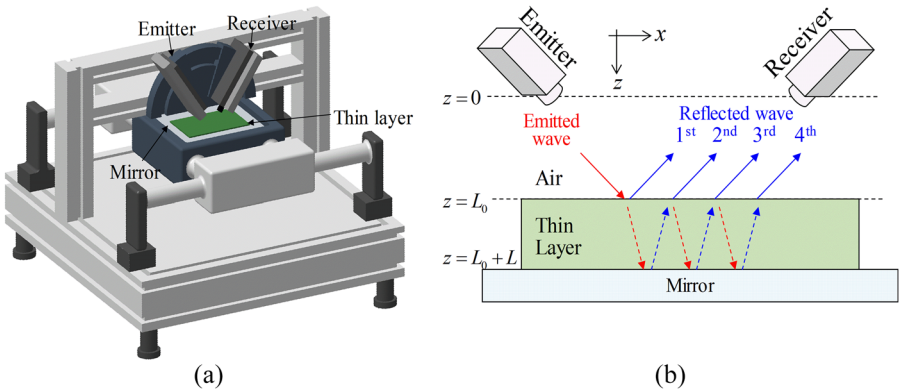

FIG. 1. (a) Experimental setup of THz pulse waves with a dielectric thin layer. (b) Schematic of the emitted and reflected THz waves via the pitch–catch mode. Waves reflected by the thin layer were measured by the receiver.

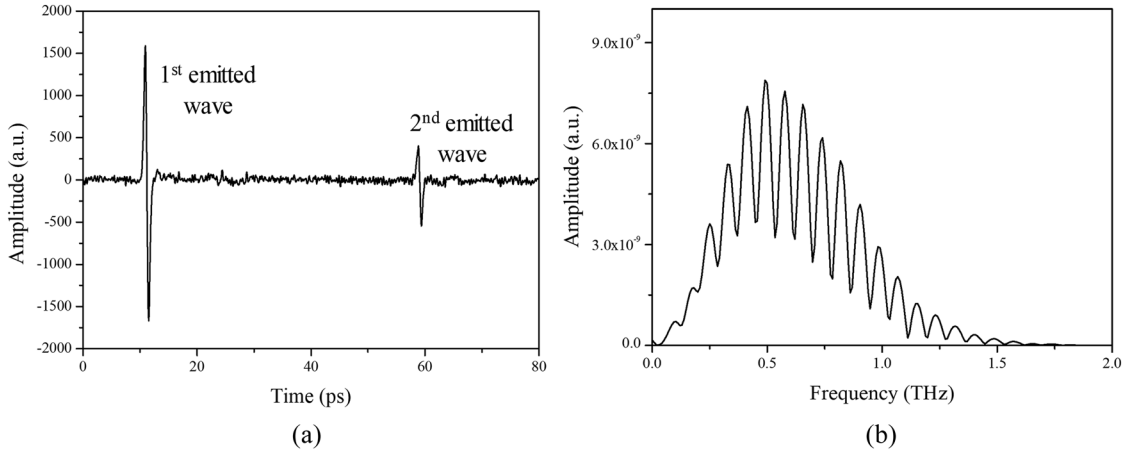

FIG. 2. (a) The transient response. (b) The autospectrum of the incident THz pulse wave from the THz emitter.

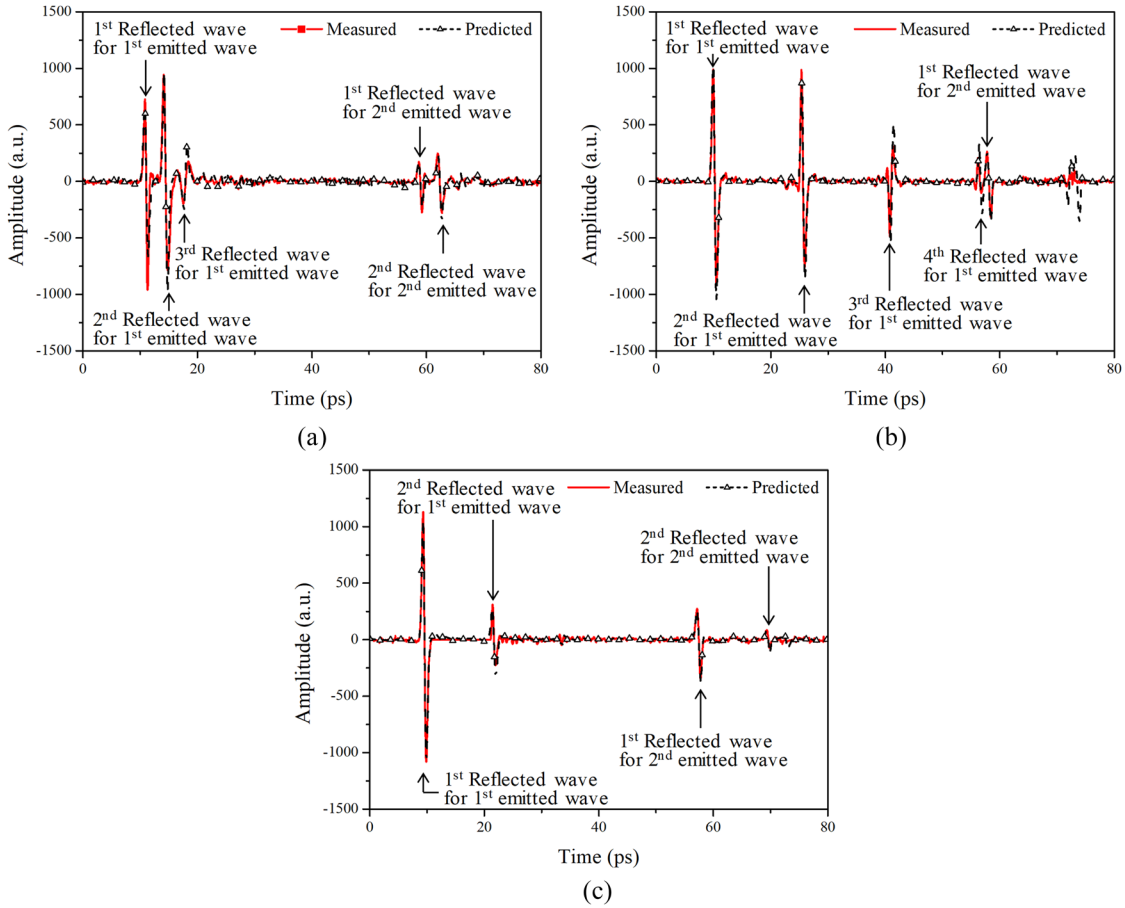

FIG. 3. The measured and predicted transient responses for different thin layers: (a) paper, (b) intrinsic silicon, and (c) p-doped silicon. Red lines denote the measured results, and dotted lines denote the predicted results. The predicted results use permittivity and conductivity obtained by the numerical calculation, as shown in Fig. 5.

where μ_0 is the air permeability. By using the proposed wave approach, the transient responses of the THz waves in the thin layer were directly predicted. The complex permittivity of each thin layer specimen was calculated and compared by using the predicted responses.

III. NONDESTRUCTIVE METHOD TO EVALUATE PROPERTIES OF THIN LAYERS USING THZ WAVES

A. Experimental setup to measure reflected THz waves

Experiments were performed using a THz-TDS imaging system (FiCOTM, Zomega Terahertz Corp., USA) which was composed of a femtosecond laser module, a THz-TDS module, and an XY fast-imaging stage.[28,29] Figure 1(a) shows the experimental setup containing the dielectric thin layer for the pitch–catch mode between the THz emitter and the receiver. The THz-TDS module was configured in a pitch–catch mode with a 45° incidence angle. Figure 1(b) shows the schematic for the emitted and reflected THz waves. The humidity condition was maintained at 1% to prevent absorption of THz waves by water vapor.

The pulse THz waves were generated from the emitter as shown in Fig. 2(a). Figure 2(b) shows the frequency spectrum of the incident wave. The emitted wave exhibited a broadband spectrum from 0.1 THz to 2.0 THz. The transfer functions were calculated and compared for the same frequency spectrum of the incident wave. Three thin layer specimens were used for the experimentations. The specimens used in the study included paper, intrinsic silicon, and p-doped silicon. The paper exhibited lower permittivity when compared with that of common semiconductors. The intrinsic silicon is a semiconductor in an initial state. The p-doped silicon is a semiconductor with added foreign atoms in the crystal lattice to change conductivity. The thickness of each specimen was 300, 720, and 540 μm, respectively. The height of the layer surface ($z = L_0$) was controlled to be identical for all specimens. The measured waves from the THz receiver were sampled uniformly with a 0.0567 ps interval for 116.077 ps (2048 data).

B. Direct measurements of the complex permittivity of the thin layer by prediction of reflected THz waves

Figure 3 shows the measured and predicted THz transient responses for different thin layers. The predicted THz waves, $\hat{E}_R$,

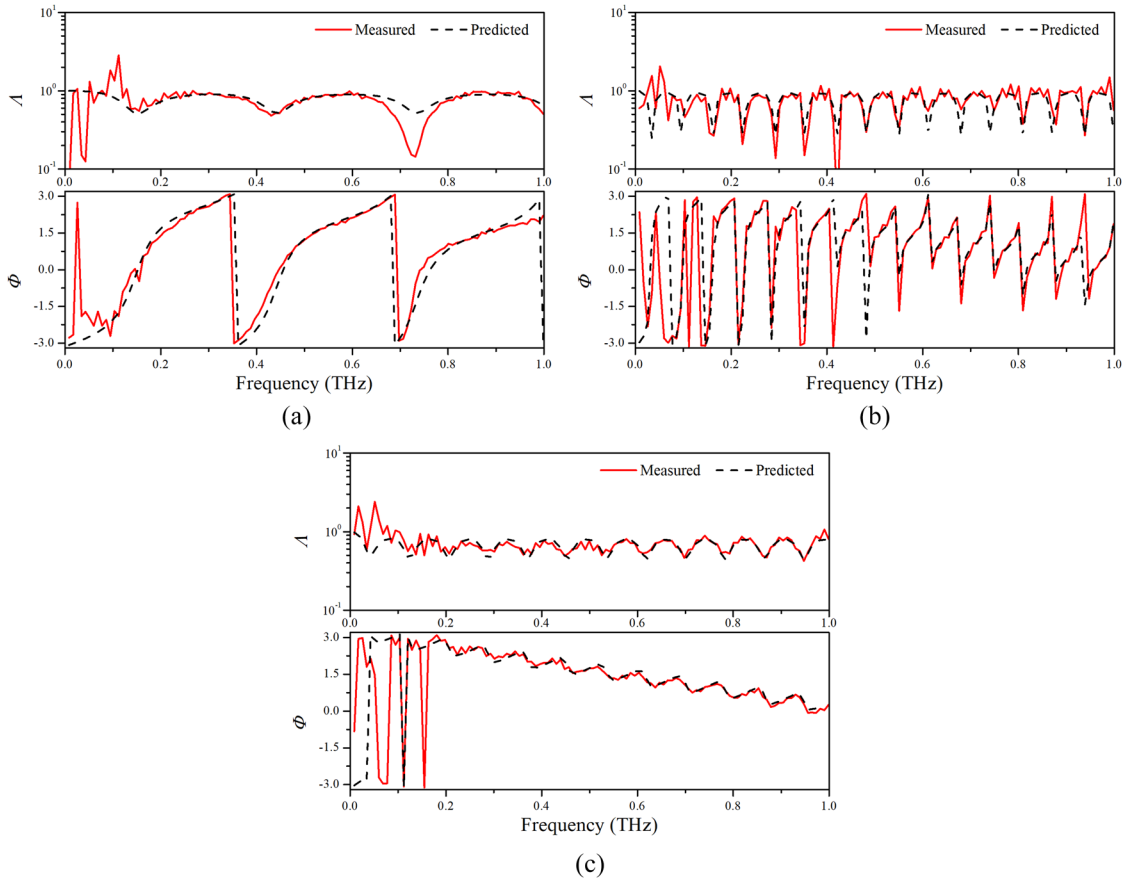

FIG. 4. The transfer functions for different thin layers: (a) paper, (b) intrinsic silicon, and (c) p-doped silicon. Red lines denote the measured results, and the dotted lines denote the predicted results. The predicted results use the same permittivity and conductivity as shown in Fig. 3.

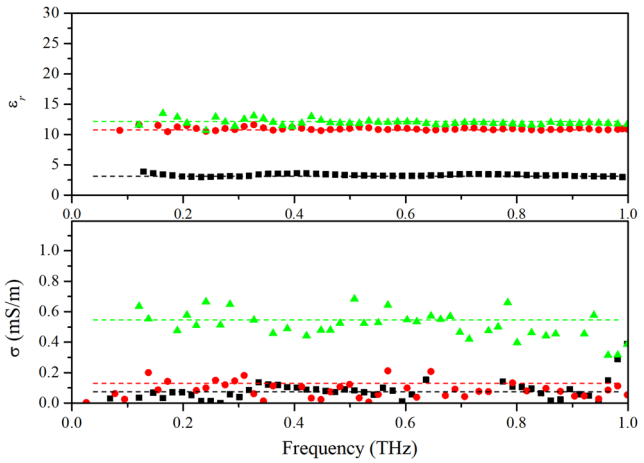

FIG. 5. The relative permittivity and conductivity with respect to the frequency for different thin layers derived by the proposed method: -■-, paper, -●-, intrinsic silicon, and -▲-, pdoped silicon.

were plotted for comparison with measured results by using the derived properties in this study. As shown in Fig. 3, the measured and predicted transient responses of all specimens showed good agreement. When compared to the paper layer, the high permittivity of the semiconductors reduced the wave speed as shown in Fig. 3(b). Figures 3(b) and 3(c) show the attenuation of the wave affected by the change in conductivity between the intrinsic silicon and p-doped silicon. The increase in the conductivity by the doping process increased the attenuation. The phase-reversed waves on several reflections were also well-reproduced without inferring the propagation path.

The transfer functions of the three specimens were calculated as shown in Fig. 4. The results used the same permittivity and conductivity as in Fig. 3. As with the transient responses, the predicted transfer showed consistency with the measured behavior. These results suggest that the theoretical procedures proposed in the study accurately represented the THz wave propagations. The magnitude and phase of transfer functions exhibited significant variations according to the permittivity and conductivity of each thin layer. These variations depending on the transfer functions allow the estimation of properties with a high resolution by the proposed numerical procedures.

Through the proposed procedure, the frequency-dependent complex permittivity was obtained by using the transfer functions in Eqs. (8) and (9). Figure 5 shows the derived properties for the three specimens. The derived permittivity was given as relative values with respect to that of air. The averaged values were used to compare the properties for each layer in 0.1–1.0 THz frequency band after neglecting large deviations. The relative permittivity, ε_r, of the paper, intrinsic silicon, and p-doped silicon was derived as 3.40, 10.88, and 11.82, respectively. The conductivities of the paper, intrinsic silicon, and p-doped silicon were derived as 0.045, 0.061, and 0.533 mS/m, respectively. The obtained properties of the layer showed close agreement with the values obtained in previous studies.[7,8,35] The permittivity of the intrinsic silicon was derived as three times larger than that of the paper. The doping process increased the conductivity of the silicon by more than ten times that of the intrinsic state. The physical correlations between the predicted values validated the proposed method.

The proposed numerical procedure based on the wave approach is an efficient method to analyze the measured behavior from tests by THz waves. This model interprets the propagating waves in thin composites without information about the inner structure. The proposed predictions allow easy integration into THz devices due to small computational costs by the direct determination of electromagnetic properties. The proposed wave approach allows prediction of the permittivity and conductivity using the simple measurement even when reflected waves are difficult to be distinguished from each other.

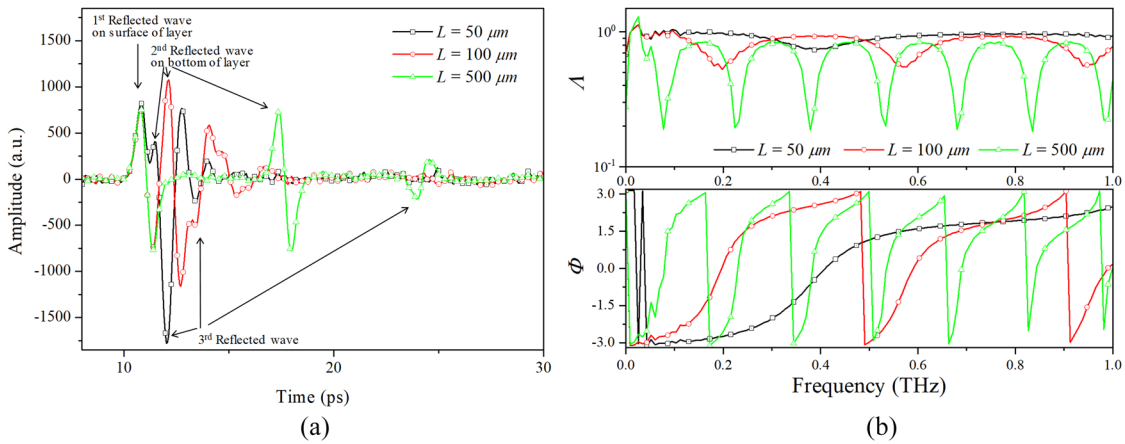

FIG. 6. (a) The predicted transient responses, and (b) the transfer functions by the proposed procedures under the condition of interferences due to the thin thickness of the layer. These interferences make it difficult to infer the propagation pathways by using the temporal calculations.

C. Discussion for the proposed evaluation method

In this paper, the material properties of the thin layers were estimated by using the transfer functions in the THz region. Researchers showed the nondestructive evaluation using the reflected waves in the time domain to evaluate the properties of composite materials.[29,31] The preceded understanding to the propagation path in the medium was required to calculate the properties through the temporal calculations. The data processing also requires considerations on the interference of the reflected waves and electronic noises.

To validate the originality of the proposed method, the wave propagation in the thin layers affected by the thickness was discussed in this section. Since the propagated wave solutions were derived by assuming harmonic responses, the transient responses in the discrete form were calculated.[36] The input wave used in the prediction was identical with the emitted signal in the experiments. The material properties were determined as those used in the previous study.[29] The permittivity was derived through the peak amplitudes, and the results were discussed with the proposed predictions in this section.

Figure 6 shows the transient responses and transfer functions predicted by using the proposed procedure for different thickness of the thin layers. The material properties of the layer were the same as in Ref. 29. As shown in Fig. 6(a), the amplitude and time of peaks with the thickness variation did not change linearly, hampering interpretation of the phase and pathway of the reflections. These interferences make it difficult to estimate the material properties based on the temporal calculations with the peaks. As shown in Fig. 6(b), the transfer functions showed distinct variations with changing thickness. The material properties were estimated from the variations via the Newton-Raphson iterations, allowing us to predict the properties of the thin layers without pre-estimating the propagation paths. The wave approach with the transfer function is advantageous on analyzing the measured behaviors among propagations which have different pathways and thickness variations.

IV. CONCLUSION

In this study, the permittivity and conductivity of thin layers were derived using the analytical model for wave propagations in the THz region. The wave approach was used to predict the propagation and reflection of the THz waves in the thin layer. The two-dimensional Helmholtz equation was applied to analyze the wave propagations. The experiments were performed with the THz-TDS imaging system. The specimens used in the experiments included paper, intrinsic silicon, and p-doped silicon. The oblique incident wave from the THz emitter was transmitted and reflected through the layer. The propagated THz wave in the thin layer was precisely reproduced by using the proposed procedures. The permittivity and conductivity were directly derived by using simple measurements of waves in the THz region. Given the direct wave prediction for layered materials, the method evaluated the properties of the thin layered materials without information about the reflective pathways of waves. In addition, the proposed approach suggests a complementary tool for understanding the measured behavior from optical imaging systems.

ACKNOWLEDGMENTS

This work was supported in part by the National Research Foundation of Korea grant, which was funded by the Korean government (Ministry of Science, ICT & Future Planning) (Grant No. 2016R1A2A1A05005392).

REFERENCES

[1] R. Dalven, Infrared Phys. **9**, 141 (1969).
[2] S. Govindarajan, T. Böscke, P. Sivasubramani, P. Kirsch, B. Lee, H.-H. Tseng, R. Jammy, U. Schröder, S. Ramanathan, and B. Gnade, Appl. Phys. Lett. **91**, 062906 (2007).
[3] C. Koops, Phys. Rev. **83**, 121 (1951).
[4] J. Sladek, V. Sladek, H.-H. Lu, and D. Young, Compos. Struct. **163**, 13 (2017).
[5] A. F. Castro, M. Valcuende, and B. Vidal, NDT&E Int. **75**, 26 (2015).
[6] S. Kharkovsky and R. Zoughi, IEEE Instrum. Meas. Mag. **10**, 26 (2007).
[7] J. Krupka, J. Breeze, A. Centeno, N. Alford, T. Claussen, and L. Jensen, IEEE Trans. Microwave Theory Tech. **54**, 3995 (2006).
[8] A. Mansingh and A. Parkash, IEEE Trans. Microwave Theory Tech. **29**, 62 (1981).
[9] Y. Jiang, Y. Ju, and L. Yang, J. Nondestr. Eval. **35**, 7 (2016).
[10] I. S. Seo and W. S. Chin, Compos. Struct. **66**, 533 (2004).
[11] U. Hasar and I. Ozbek, J. Electromagn. Waves Appl. **25**, 2100 (2011).
[12] T. Chang, X. Zhang, X. Zhang, and H.-L. Cui, Appl. Opt. **56**, 3287 (2017).
[13] K. Kawase, Y. Ogawa, Y. Watanabe, and H. Inoue, Opt. Express **11**, 2549 (2003).
[14] S. Wietzke, C. Jördens, N. Krumbholz, B. Baudrit, M. Bastian, and M. Koch, J. Eur. Opt. Soc.–Rapid Publ. **2**, 07013 (2007).
[15] C. Jördens, M. Scheller, S. Wietzke, D. Romeike, C. Jansen, T. Zentgraf, K. Wiesauer, V. Reisecker, and M. Koch, Compos. Sci. Technol. **70**, 472 (2010).
[16] H. Zhang, S. Sfarra, K. Saluja, J. Peeters, J. Fleuret, Y. Duan, H. Fernandes, N. Avdelidis, C. Ibarra-Castanedo, and X. Maldague, J. Nondestr. Eval. **36**, 34 (2017).
[17] X. Zhang, Phys. Med. Biol. **47**, 3667 (2002).
[18] F. Rutz, T. Hasek, M. Koch, H. Richter, and U. Ewert, Appl. Phys. Lett. **89**, 221911 (2006).
[19] C. Jördens, S. Wietzke, M. Scheller, and M. Koch, Polym. Test. **29**, 209 (2010).
[20] D. M. Mittleman, J. Appl. Phys. **122**, 230901 (2017).
[21] I. Amenabar, F. Lopez, and A. Mendikute, J. Infrared, Millimeter, Terahertz Waves **34**, 152 (2013).
[22] B. E. Knighton, R. Tanner Hardy, C. L. Johnson, L. M. Rawlings, J. T. Woolley, C. Calderon, A. Urrea, and J. A. Johnson, J. Appl. Phys. **125**, 144101 (2019).
[23] H. J. Joyce, J. L. Boland, C. L. Davies, S. A. Baig, and M. B. Johnston, Semicond. Sci. Technol. **31**, 103003 (2016).
[24] P. D. Cunningham, N. N. Valdes, F. A. Vallejo, L. M. Hayden, B. Polishak, X.-H. Zhou, J. Luo, A. K.-Y. Jen, J. C. Williams, and R. J. Twieg, J. Appl. Phys. **109**, 043505 (2011).
[25] F. D'Angelo, Z. Mics, M. Bonn, and D. Turchinovich, Opt. Express **22**, 12475 (2014).
[26] A. Podzorov and G. Gallot, Appl. Opt. **47**, 3254 (2008).
[27] T. Inagaki, B. Ahmed, I. D. Hartley, S. Tsuchikawa, and M. Reid, J. Infrared, Millimeter, Terahertz Waves **35**, 949 (2014).
[28] S.-H. Park, J.-W. Jang, and H.-S. Kim, J. Micromech. Microeng. **25**, 095007 (2015).
[29] C.-H. Ryu, S.-H. Park, D.-H. Kim, K.-Y. Jhang, and H.-S. Kim, Compos. Struct. **156**, 338 (2016).
[30] C. Stoik, M. Bohn, and J. Blackshire, NDT&E Int. **43**, 106 (2010).
[31] M. Sudo, J. Takayanagi, and H. Ohtake, J. Infrared, Millimeter, Terahertz Waves **37**, 1139 (2016).
[32] W.-C. Wang, *Electromagnetic Wave Theory* (Wiley, New York, 1986).
[33] H. J. Eom, *Electromagnetic Wave Theory for Boundary-Value Problems* (Springer, 2004).
[34] J. Park, J. Sound Vib. **288**, 57 (2005).
[35] M. S. Shur, *Handbook Series on Semiconductor Parameters* (World Scientific, 1996), Vol. 1.
[36] U. Lee, *Spectral Element Method in Structural Dynamics* (John Wiley & Sons, 2009).